Exchange Coupling between Siroheme and [4Fe-4S] Cluster in *E. Coli* Sulfite Reductase. Mössbauer Studies and Coupling Models for a 2-Electron Reduced Enzyme State and Complexes with Sulfide

Jodie A. Christner,[†] Eckard Münck,*[†] Thomas A. Kent,[†] Peter A. Janick,[§] John C. Salerno,[§,‡] and Lewis M. Siegel[§]

Contribution from the Gray Freshwater Biological Institute, University of Minnesota, Navarre, Minnesota 55392, and the Department of Biochemistry, Duke University Medical Center and Veterans Administration Hospital, Durham, North Carolina 27705. *Received February 24, 1984*

Abstract: Recent Mössbauer and EPR studies of the hemoprotein subunit (SiR) of *E. coli* sulfite reductase have shown that the siroheme and the [4Fe-4S] cluster are exchange coupled in a variety of states. Mössbauer studies of 2-electron-reduced SiR in the presence of 0.1 M guanidinium sulfate, $SiR^{2-}/(Gdm)_2SO_4$, and of complexes of SiR with sulfide are reported. $SiR^{2-}/(Gdm)_2SO_4$ exhibits an EPR signal with g values characteristic of a system with electronic spin $S = {}^3/_2$. Mössbauer studies had indicated problems with such an interpretation. It is shown here that the siroheme iron of $SiR^{2-}/(Gdm)_2SO_4$ is high-spin ferrous ($S_h = 2$). With this firm assignment a spin coupling model is developed which is in accord with the EPR and Mössbauer data. In this model the reduced iron sulfur cluster, with cluster spin $S_c = {}^1/_2$, is exchange coupled to the siroheme iron, $\hat{H}_{ex} = J(\vec{S}_c \cdot \vec{S}_h)$, where J is an effective coupling constant. J/D is determined to be -0.22, where D is the zero-field splitting parameter of the heme ($D > 0$ and $D \simeq 5$–15 cm^{-1}). It is discussed how J is related to the coupling constant which characterizes the presumed bond between the siroheme iron and one iron subsite of the cluster. The model fits the EPR data of a variety of SiR complexes and of 2-electron-reduced spinach nitrite reductase. The similarity of the observed g values with those of an $S = {}^3/_2$ system turns out to be fortuitous. The Mössbauer spectra of oxidized SiR with sulfide show that the heme iron is low-spin ferric ($S_h = {}^1/_2$) and that the [4Fe-4S] cluster is in the 2+ oxidation state. Upon addition of one electron per siroheme the [4Fe-4S] cluster is reduced to the 1+ oxidation state ($S_c = {}^1/_2$) while the heme iron remains low-spin ferric. Mössbauer spectra recorded at 4.2 K in a 6.0-T magnetic field show that both the heme and the cluster reside in a diamagnetic environment. The diamagnetism results from exchange interactions, $\hat{H}_{ex} = J(\vec{S}_c \cdot \vec{S}_h)$, between the heme iron and the cluster. The high-field studies show that $J > 6$ cm^{-1}.

The NADPH-sulfite reductase of *Escherichia coli* is a large ($M_r = 685\,000$) oligomeric hemoflavoprotein ($\alpha_8\beta_4$) which catalyzes the 6-electron reduction of sulfite to sulfide or of nitrite to ammonia. The protein can be dissociated in 4 M urea, and the β subunits ($M_r = 54\,000$) can be separated by DEAE-cellulose chromatography. The β subunit, termed SiR, is monomeric and contains one siroheme (an iron isobacteriochlorin) and one [4Fe-4S] cluster.[1,2] It can catalyze both sulfite and nitrite reduction at high rates if supplied with a suitable electron donor.

In a series of publications,[3-9] we have shown that the iron-sulfur cluster and the siroheme are chemically linked as witnessed by the observation of exchange interactions. These exchange interactions have been observed thus far in nine different oxidation and complexation states of the enzyme. The uncomplexed enzyme has three stable oxidation states.[10] SiR^0 and SiR^{2-} have an odd number of electrons, i.e., they are Kramers systems, and exhibit intense EPR signals at temperatures below 30 K. SiR is capable of complexing exogeneous ligands such as CO, CN^-, SO_3^{2-}, NO_2^-, S^{2-}, and NO. All of these complexes can be studied in two or three different oxidation states. Although the siroheme iron and the [4Fe-4S] cluster are chemically linked and although the electronic magnetic moment reflects the exchange-coupled unit, both the siroheme and the iron-sulfur center retain most of the spectroscopic features which are characteristic of the uncoupled prosthetic groups. For instance, the Mössbauer quadrupole splittings and the isomer shifts are typical of those observed for other hemes and [4Fe-4S] clusters. In particular, characteristic oxidation states are spectroscopically clearly discernible. Thus, the siroheme iron is observed in the Fe^{3+} and Fe^{2+} oxidation states typical of other iron porphyrins, in both high-spin and low-spin states. The iron-sulfur cluster occurs in either the 2+ oxidation state ($[4Fe\text{-}4S]^{2+}$, electronic spin $S_c = 0$) or the reduced 1+ state. In uncoupled systems, the latter normally exhibits a "$g = 1.94$" EPR signal.

In SiR^0, SiR^{1-}, SiR^0-CN, and SiR^{1-}-NO, the [4Fe-4S] cluster is in the 2+ oxidation state.[3,5] Despite the fact that $[4Fe\text{-}4S]^{2+}$ clusters are in general diamagnetic, we have observed magnetic hyperfine interactions for all four cluster iron sites in the low-temperature Mössbauer spectra. (Pure diamagnetic states can exhibit no such magnetic hyperfine interactions.) We have shown that these interactions reflect exchange coupling between the cluster and the paramagnetic siroheme iron. For SiR^0 we have proposed a novel coupling mechanism[9,11] which explains the experimental data qualitatively quite well. In this model, exchange coupling between the siroheme iron and one iron of the [4Fe-4S] cluster perturbs the (strong) internal spin coupling of the cluster, mixing excited triplet states into the ground state. By this mechanism the cluster ground state acquires paramagnetic properties. From a comparison of the observed magnetic hyperfine interactions in SiR^0-CN and SiR^{1-}-NO we have deduced that the exchange interaction in the nitrosyl complex is one order of

[†] University of Minnesota, Gray Freshwater Biological Institute, Navarre, Minnesota 55392.
[§] Duke University Medical Center and VA Hospital, Durham, North Carolina 27705.
[‡] Present Address: Department of Biology, Rennselaer Polytechnic Institute, Troy, NY 12181.

(1) Siegel, L. M.; Davis, P. S. *J. Biol. Chem.* **1974**, *249*, 1572-1596.
(2) Siegel, L. M.; Rueger, D. C.; Barker, M. J.; Krueger, R. J.; Orme-Johnson, N. R.; Orme-Johnson, W. M. *J. Biol. Chem.* **1982**, *257*, 6343-6350.
(3) Christner, J. A.; Münck, E.; Janick, P. A.; Siegel, L. M. *J. Biol. Chem.* **1981**, *256*, 2098-2101.
(4) Janick, P. A.; Siegel, L. M. *Biochemistry* **1982**, *21*, 3538-3547.
(5) Christner, J. A.; Münck, E.; Janick, P. A.; Siegel, L. M. *J. Biol. Chem.* **1983**, *258*, 11147-11156.
(6) Christner, J. A.; Janick, P. A.; Siegel, L. M.; Münck, E. *J. Biol. Chem.* **1983**, *258*, 11157-11164.
(7) Janick, P. A.; Rueger, D. C.; Krueger, R. J.; Barker, M. J.; Siegel, L. M. *Biochemistry* **1983**, *22*, 396-408.
(8) Janick, P. A.; Siegel, L. M. *Biochemistry* **1983**, *22*, 504-514.
(9) Münck, E. In "Iron Sulfur Proteins"; John Wiley and Sons: New York; 1982, pp 147-175.
(10) We have designated these states as SiR^0, SiR^{1-}, and SiR^{2-} for the oxidized, 1-electron-reduced, and 2-electron-reduced enzyme states, respectively. To describe the oxidation states of complexes with added ligands, we use a similar nomenclature, e.g., SiR^{2-}-CO designates the carbon monoxide complex of 2-electron-reduced SiR.
(11) Christner, J. A. Ph.D. Thesis, University of Minnesota, 1983.

0002-7863/84/1506-6786$01.50/0 © 1984 American Chemical Society

magnitude stronger than that in the cyanide complex.[5] The strength of the exchange interaction has not been determined for any of the states studied thus far. (Progress in this area will require a detailed understanding of the electronic structure of [4Fe–4S] clusters.)

Janick and Siegel[4,8] have shown that 2-electron-reduced SiR exhibits three different types of EPR signals. In SiR^{2-}–CO and SiR^{2-}–CN and in SiR^{2-} prepared in 60% dimethyl sulfoxide, for instance, signals with $g \simeq 1.91$, 1.93, and 2.03 are observed. In these complexes the heme iron is in the low-spin ($S_h = 0$) ferrous state and the magnetic properties of the $[4Fe–4S]^{1+}$ cluster are essentially the same as those of a cluster which is not coupled to the siroheme.[6] We refer to this state as the "$g = 1.94$" state. Uncomplexed SiR^{2-} exhibits a majority species with $g = 2.53$, 2.29, and 2.07. The nature of this signal is not yet fully understood. It is clear, however, that the siroheme iron and the cluster are exchange coupled in the SiR^{2-} species giving rise to this signal. In the following, we will refer to this state of the enzyme as the "$g = 2.29$" state.

In the presence of (potential) weak field heme ligands, such as halides or formate, or in the presence of certain chaotropic agents, such as guanidinium (Gdm) salts, a new type of EPR signal becomes the major species for SiR^{2-}. For instance, addition of $(Gdm)_2SO_4$ (100 mM) or KCl (5 mM) to SiR^{2-} leads to the diminution of the "$g = 2.29$" species and the concomitant appearance of signals at $g_1 = 4.88$, $g_2 = 3.31$, and $g_3 = 2.07$ (in Gdm_2SO_4) and $g_1 = 5.08$, $g_2 = 2.55$, and $g_3 \simeq 2$ (in KCl). Similar signals have also been reported as majority EPR species for 2-electron-reduced spinach nitrite reductase[12] and are also seen as minor species in unligated SiR^{2-}. These g values are readily explained within the framework of a spin Hamiltonian for an $S = {}^3/_2$ system (see footnote 3 of ref 5). Therefore, in the past we referred to these species as "$S = {}^3/_2$" type. Mössbauer studies[5,6] of the reduced states of SiR have shown that the electronic structure of iron–sulfur clusters is virtually the same in the "$g = 1.94$", "$g = 2.29$", and "$S = {}^3/_2$" forms. The cluster is formally in the 1+ oxidation state and the observed Mössbauer parameters, are quite similar to those reported for the [4Fe–4S] ferredoxin from *Bacillus stearothermophilus*.[13] What came to us as a surprise was the observation that the magnetic hyperfine interactions observed for the $[4Fe–4S]^{1+}$ cluster are the same in all three states, despite the fact that the expectation value of the spin, $\langle S \rangle$, should be more than twice as large for the "$S = {}^3/_2$" species than for the "$g = 1.94$" species. Since the magnetic hyperfine interactions are proportional to $\langle S \rangle$, a substantially larger splitting was thus expected for the "$S = {}^3/_2$" species. In our previous studies, we have not been able to identify the spin states of the iron(II) siroheme in the "$g = 2.29$" and "$S = {}^3/_2$" species. In this paper we will show that the heme iron is high-spin ferrous ($S_h = 2$) in the "$S = {}^3/_2$" species. This knowledge allows us to develop a spin-coupling model that will explain the EPR as well as Mössbauer data. Our results will show that the similarity of the "$S = {}^3/_2$" type species with a real $S = {}^3/_2$ system is fortuitous and that the "$S = {}^3/_2$" signals result from weak exchange coupling of the cluster with the high-spin ferrous heme. In the following we will replace the phrase "$S = {}^3/_2$" state with "$g_1 = 5$" or, specifically, with "$g_1 = 4.88$" state.

We will also report Mössbauer studies on two complexes of SiR with sulfide. We will show that the heme iron of the 1-electron-reduced complex, SiR^{1-}–S^{2-}, is low-spin ferric ($S_h = {}^1/_2$) and that the cluster is in the $S_c = {}^1/_2$ ($g = 1.94$) state. The system is exchange coupled to give a diamagnetic ground state.

Materials and Methods

E. coli K12 cells were grown as previously described,[14] with 0.5 mg per ^{57}Fe (95% enrichment, New England Nuclear). Sulfite reductase hemoflavoprotein complex was purified as described by Siegel et al.,[14] and the β subunit (SiR) was isolated by using the method of Siegel and Davis.[1] Enzyme concentration was determined by using $\epsilon_{591} = 1.8 \times 10^4$ M^{-1} cm^{-1}.[14] (All the studies reported in this work were performed with ^{57}Fe-enriched SiR.)

SiR^{2-} in $(Gdm)_2SO_4$ was prepared by photoreducing[15] 150-μL aliquots of an anaerobic solution containing 300 μM SiR, 50 μM deazaflavin, 10 mM EDTA, and 0.1 M $(Gdm)_2SO_4$ in 50 mM potassium phosphate (pH 7.7). One aliquot of this solution was introduced into a Mössbauer cup (9-mm i.d.) in a Thunberg tube under Ar, and photoreduction was performed by illuminating the solution from above with a sealed beam lamp. In parallel, 150 μL of the same solution was photoreduced in an EPR tube to permit us to monitor the state of reduction both optically and by EPR (after freezing the final reduced solution in liquid N_2). Both samples were cooled during illumination in an ice bath. After reduction was complete (1.5–2 h), the Mössbauer sample was frozen by immersing the Thunberg tube in liquid nitrogen.

The Mössbauer sample of reduced SiR ligated to S^{2-} was prepared by photoreducing an anaerobic solution of 200 μM SiR, 50 μM deazaflavin, 10 mM EDTA, and 20 mM Na_2S in an EPR tube to allow rapid binding of the ligand to the siroheme. The sample was buffered by 200 mM potassium phosphate adjusted to give a pH of 7.7 upon addition of the sulfide. Then 150 μL of the partially reduced SiR^{2-} was anaerobically transferred to each of two Mössbauer cups in a Thunberg tube under Ar and to an anaerobic EPR tube. The samples were further illuminated and monitored as described above until the optical spectrum of the photoreduced enzyme indicated that it was largely in the "form 2", or EPR silent (SiR^{1-}–S^{2-}), state described by Siegel and Janick.[8] Further photoreduction of such optically dense SiR–S^{2-} samples to the "form 3", or SiR^{2-}–S^{2-}, state has not yet proved possible. Two such samples were placed end to end in the Mössbauer spectrophotometer for analysis.

The Mössbauer sample of oxidized SiR–S^{2-} was prepared by photoreducing 450 μL of an anaerobic solution of 300 μM SiR, 50 μM deazaflavin, 10 mM EDTA, and 20 mM S^{2-} in an EPR tube to allow formation of the SiR–S^{2-} complex as determined by the optical spectrum. The sample was oxidized by the addition of 20 μL of air-saturated buffer. Then 300 μL of the sample was transferred to a single Mössbauer cup and frozen while the remaining sample was frozen in liquid nitrogen for EPR studies.

Optical spectroscopy was performed on an Aminco DW-2 dual beam spectrophotometer. EPR spectra were recorded as described previously[4,8] with a Varian E9 spectrometer equipped with an Air Products He gas transfer cryostat. Spin concentrations were determined by quantitation against a cupric EDTA standard.

The Mössbauer spectrometers were of the constant acceleration type. For measurements in zero field or in applied fields of 60 mT, a Janis Super Vari Temp Dewar was used. The high-field spectra were recorded in a second Janis Research Co. Dewar which was equipped with an American Magnetics superconducting magnet. For measurements in the Super Vari Temp Dewar, the source, 60 mCi of ^{57}Co in rhodium, was mounted outside the Dewar and kept at room temperature. For the high-field measurements, the source was mounted on a vertical suspension system and kept at the same temperature as the sample. The isomer shifts, δ, are quoted relative to the center of the spectrum of metallic iron recorded at room temperature.

Results and Discussion

Mössbauer Studies of SiR^{2-} in Guanidinium Sulfate. We have studied with Mössbauer and EPR spectroscopy a sample of ^{57}Fe-enriched SiR^{2-} containing 0.1 M $(Gdm)_2SO_4$ in potassium phosphate, pH 7.7. The EPR spectra show the presence of a "$g_1 = 5$" type species with $g_1 = 4.88$, $g_2 = 3.31$, and $g_3 = 2.07$ (ca. 0.7 spin/siroheme), a "$g = 1.94$" species ($\approx$0.15 spin/siroheme), and a weak signal of the "$g = 2.29$" species ($\approx$0.07 spin/siroheme). The quoted spin concentrations were obtained from an EPR sample which was prepared parallel to the Mössbauer sample. The accuracy of the spin quantitations is at best $\pm$15% for each species. The EPR spectrum of the sample was very similar to that shown in Figure 4B of ref 4, except that this sample had a "$g = 1.94$" signal that was 3 times stronger.

Figure 1 shows a Mössbauer spectrum of $SiR^{2-}/(Gdm)_2SO_4$ taken at 110 K in the absence of an applied magnetic field. The spectrum is readily understood in the context of our earlier studies. The dashed line shows the spectrum of the $[4Fe–4S]^{1+}$ cluster of SiR^{2-}–CN; it consists of two nested doublets of equal intensity. The outer doublet belongs to two equivalent iron sites of ferrous

(12) Wilkerson, J. O.; Janick, P. A.; Siegel, L. M. *Biochemistry* **1983**, *22*, 5048–5054.
(13) Middleton, P.; Dickson, D. P. E.; Johnson, C. E.; Rush, J. D. *Eur. J. Biochem.* **1978**, *88*, 135–141.
(14) Siegel, L. M.; Murphy, M. J.; Kamin, H. *J. Biol. Chem.* **1973**, *248*, 251–264.
(15) Massey, V.; Hemmerich, P. *Biochemistry* **1978**, *17*, 9–17.

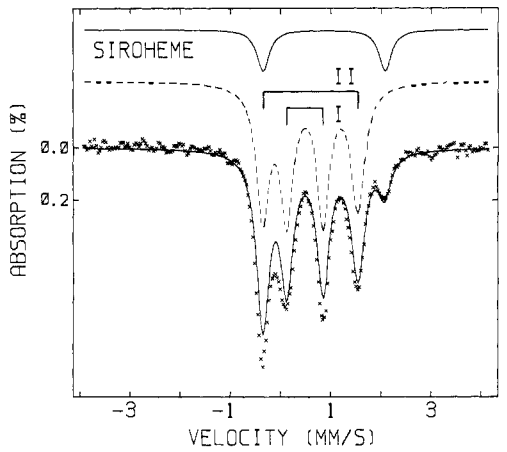

Figure 1. Mössbauer spectrum of fully reduced SiR in guanidinium sulfate recorded at 110 K in zero field (crosses). Contributions (see text) from the siroheme iron (solid curve) and from the [4Fe–4S] cluster (dashed curve) are shown with base lines displaced above that of the data. Their sum is displayed as the solid curve plotted over the data and is scaled to 92% of the total absorption.

character while the inner doublet represents two sites with ferric character (for details see the Discussion in ref 6). A third doublet, contributed by the siroheme iron, is indicated by the solid line drawn above the data of Figure 1. This doublet is only observed when "g_1 = 5" species are present. (The siroheme irons of the "g = 2.29" and "g = 1.94" species have quite different doublets.) Analysis of the spectra of Figure 1 reveals that 12% of the total ^{57}Fe absorption belongs to this doublet. Since SiR contains one siroheme and one [4Fe–4S] cluster this result suggests that 60% of the molecules in the sample belong to the "g_1 = 4.88" species. This value is in reasonable agreement with the EPR data. According to the EPR spectra the sum of the "g = 2.29" and "g = 1.94" species is approximately 20% of the total spin concentration. As pointed out above, the $[4Fe–4S]^{1+}$ clusters for all EPR-active species discussed here display the same pattern of quadrupole doublets. Our analysis of the spectrum of Figure 1 shows that 80% of the total ^{57}Fe concentration belongs to the two doublets indicated by the dashed curve. This suggests that the sample contains the "g_1 = 4.88" species at 60% of the total ^{57}Fe concentration whereas the sum of the "g = 2.29" and "g = 1.94" species contributes approximately 40%. The solid line through the data of Figure 1 is the sum of the siroheme (12%) and the $[4Fe–4S]^{1+}$ cluster (80%) contributions. The remaining 8% of the absorption is not well-defined; it belongs to the siroheme iron of the "g = 2.29" and "g = 1.94" species.

The doublet which we have assigned to the siroheme iron has a quadrupole splitting, ΔE_Q = (2.40 ± 0.10) mm/s, and an isomer shift, δ = (0.88 ± 0.05) mm/s, at 110 K. In a plot of ΔE_Q vs. δ the high-spin ferrous state occupies a unique region, clearly separated from other spin and oxidation states of iron (see Figures 1 and 2 of ref 16). The parameters observed here fall squarely into this region and thus establish unambiguously that the siroheme iron of $SiR^{2-}/(Gdm)_2SO_4$ is high-spin ferrous (electronic spin S_h = 2). The value of ΔE_Q of the siroheme iron is temperature dependent, with ΔE_Q = 2.20 mm/s at 175 K.

At 110 K the electronic spin relaxation rate is fast compared with the nuclear precession frequencies. Consequently, magnetic hyperfine interactions are not observed. At 4.2 K, however, the electronic spins of the "g_1 = 4.88", "g = 2.29", and "g = 1.94" species relax slowly and well developed magnetic hyperfine patterns are observed. Figure 2 shows a 4.2 K Mössbauer spectrum (hash marks) recorded in a magnetic field of 60 mT applied parallel to the observed γ-radiation. Considering that the sample contains three species, albeit with the "g_1 = 4.88" form dominant, it would be futile to attempt a decomposition of the spectrum (9–15 subspectra would be involved[17]). However, the essential information

(16) Maeda, Y. *J. Phys. (Orsay Fr.)* **1979**, *40*, C2-514–522.

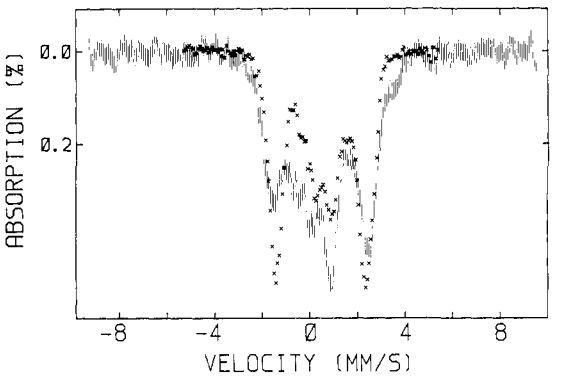

Figure 2. Mössbauer spectrum (4.2 K) of SiR^{2-} in $(Gdm)_2SO_4$. The data (hash marks) were taken in a 60-mT parallel applied field. For comparison, the corresponding spectrum[6] (crosses) of the $[4Fe–4S]^+$ cluster of SiR^{2-}–CO is plotted as 80% of the total absorption.

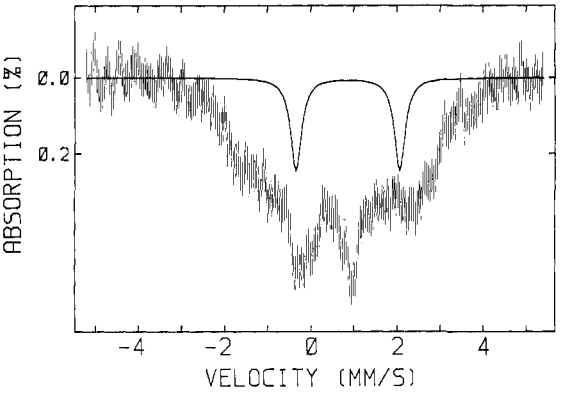

Figure 3. Zero-field spectrum of $SiR^{2-}/(Gdm)_2SO_4$ taken at 4.2 K. The solid curve is the 110 K spectrum of the siroheme (scaled to 12% total absorption) (Figure 1), with a correction made for the second-order Doppler shift.

can be extracted by comparing the data with the corresponding spectrum of the $[4Fe–4S]^{1+}$ cluster of SiR^{2-}–CO. (We have analyzed the spectra of SiR^{2-}–CO in detail.[6] We have also shown that the clusters of SiR^{2-}–CN and SiR^{2-}–CO are essentially identical.) The full crosses in Figure 2 show the spectrum of the $[4Fe–4S]^{1+}$ cluster of SiR^{2-}–CO, scaled to represent 80% of the total absorption of the $SiR^{2-}/(Gdm)_2SO_4^{2-}$ spectrum. The general features of the spectra are quite similar. In particular, it is remarkable that the magnetic splittings observed for the [4Fe–4S]$^{1+}$ cluster of the "g_1 = 4.88" species are essentially the same as those observed for the cluster of the "g = 1.94" species. This observation implies that the internal magnetic fields, H_{int}, at the ^{57}Fe nuclei of the iron–sulfur cluster are the same regardless of whether SiR^{2-} is in the "g_1 = 4.88" or "g = 1.94" state.

The Mössbauer parameters of the siroheme of the "g_1 = 4.88" species leave no doubt that the heme is high-spin ferrous. Since an isolated high-spin ferrous ion has integer electronic spin it cannot have a permanent magnetic moment in the absence of an applied magnetic field, i.e., the expectation value of the electronic spin would be zero. Therefore (see below), the zero-field Mössbauer spectrum of the siroheme would consist of a quadrupole doublet as observed at 110 K, with, perhaps, a slightly larger ΔE_Q. Figure 3 shows a spectrum of $SiR^{2-}/(Gdm)SO_4$ recorded at 4.2 K in zero field. The solid line is the quadrupole doublet of the siroheme iron, normalized to 12% of the total absorption, as observed in Figure 1. Obviously the experimental spectrum does not contain such a doublet, and we conclude that the siroheme spectrum must exhibit the paramagnetic hyperfine structure.[18]

(17) Presently B. M. Hoffman, J. Cline, P. A. Janick, and L. M. Siegel are studying the "g_1 = 4.88" species with electron nuclear double resonance spectroscopy. Preliminary data show the presence of well-defined resonances attributable to ^{57}Fe. By combining the results of both spectroscopies further analysis of the spectra seems feasible in the near future.

Thus, the heme must belong to an electronic system of half-integer electronic spin, i.e., it is magnetically coupled to the $[4Fe-4S]^{1+}$ cluster. The same observation holds for the data of Figure 2; the siroheme spectrum exhibits magnetic features. (We are convinced that the shoulder at +3.6 mm/s belongs to the heme spectrum.)

We have also recorded spectra at 4.2 K in a 60-mT transverse field and in a parallel field of 6.0 T. Again the spectra of the [4Fe–4S] cluster of the "g_1 = 4.88" species are very similar to the corresponding ones of the SiR^{2-}–CO.

Theory for "g_1 = 5" State. The EPR data of SiR^{2-} in $(Gdm)_2SO_4$ are strongly suggestive of an $S = {}^3/_2$ spin system. As pointed out previously (see footnote 3 in ref 5), the g values observed at g = 4.88, 3.31, and 2.08 can be described quite satisfactorily in the framework of an $S = {}^3/_2$ spin Hamiltonian. What has puzzled us, and we have discussed this at length,[5] is the observation that the magnetic splittings observed in the 4.2 K Mössbauer spectra of the [4Fe–4S] cluster of the "g_1 = 5" type species are practically identical with those observed when the cluster is in the $S = {}^1/_2$ ("g = 1.94") state. In the spin Hamiltonian formalism the magnetic hyperfine interactions of the ^{57}Fe nucleus (magnetic moment $g_n\beta_n$ I) with its environment can be described by $\hat{H} = -g_n\beta_n \vec{\mathbf{H}}_{int}\cdot\vec{\mathbf{I}}$ where $\vec{\mathbf{H}}_{int} = -\langle\vec{\mathbf{S}}\rangle\cdot\tilde{\mathbf{A}}/g_n\beta_n$ is the internal magnetic field, $\tilde{\mathbf{A}}$ is the magnetic hyperfine coupling tensor, and $\langle\vec{\mathbf{S}}\rangle$ is the expectation value of the electronic spin S. We have discussed previously[5] that $\langle\vec{\mathbf{S}}\rangle$ should be about 2.5 times larger for the "g_1 = 5" type species than for the $S = {}^1/_2$ states of either the "g = 2.29" or the "g = 1.94" species. We have also suggested that the similarity of the Mössbauer spectra of the [4Fe–4S] cluster in the "$S = {}^3/_2$" and $S = {}^1/_2$ states is a crucial experimental observation which a spin-coupling model has to explain. In the following we develop a simple coupling model which provides an explanation for the experimental observations. A similar model describing weak coupling of the ferrous ion and a semiquinone radical in the reaction center of *Rhodopseudomonas sphaeroides* has been discussed by Butler et al.[19]

The model we wish to discuss takes into account the fact that the siroheme iron of the "g_1 = 5" type species is high-spin ferrous (S_h = 2). The electronic ground state of a high-spin ferrous ion can often be described by the S_h = 2 spin Hamiltonian

$$\hat{H} = D\left[S_{hz}^2 - 2 + \frac{E}{D}(S_{hx}^2 - S_{hy}^2)\right] + \beta(\vec{\mathbf{S}}_h\cdot\tilde{\mathbf{g}}_h\cdot\vec{\mathbf{H}}) = \hat{H}_{ZF} + \beta(\vec{\mathbf{S}}_h\cdot\tilde{\mathbf{g}}_h\cdot\vec{\mathbf{H}}) \quad (1)$$

where D and E are parameters describing the zero-field splitting of the spin quintet and where $\tilde{\mathbf{g}}_h$ is the g tensor. If excited orbital states are sufficiently removed in energy from the ground state, eq 1 can be derived by second-order perturbation theory. In this approximation two of the three g values are related to D and E by[19,21]

$$g_{hx} = g_{hz} - (2D/\lambda)(1 - E/D)$$
$$g_{hy} = g_{hz} - (2D/\lambda)(1 + E/D) \quad (2)$$

where $\lambda \approx -80$ cm^{-1} is the spin–orbit coupling constant. D values for high-spin ferrous hemes are in the range 5–10 cm^{-1} (see below). The left column of Figure 4 depicts the energy levels of the high-spin ferrous ion for $D > 0$ and $E = 0$ as well as $E \neq 0$. For $E \neq 0$ the zero-field splitting term mixes the $M_h = \pm 2$ levels into the $M_h = 0$ ground singlet.

The ground state of the [4Fe–4S] cluster in the 1+ oxidation state has a cluster spin $S_c = {}^1/_2$ which results from strong antiferromagnetic coupling among the four constituent iron atoms.

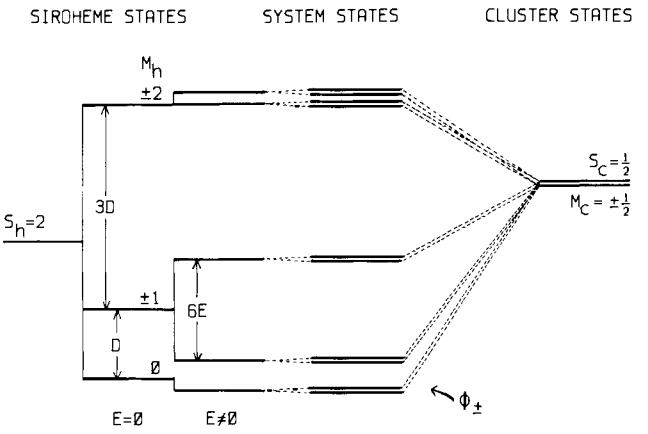

Figure 4. Proposed energy levels of the exchange-coupled system observed for the "g_1 = 5" type species of SiR^{2-}.

The lowest lying excited states of the [4Fe–4S] cluster are approximately 50–100 cm^{-1} above the ground doublet; we will ignore these states here. In the presence of an applied magnetic field we describe the Zeeman splitting of the $S_c = {}^1/_2$ ground state by

$$\hat{H}_z = \beta(\vec{\mathbf{S}}_c\cdot\tilde{\mathbf{g}}_c\cdot\vec{\mathbf{H}}) \quad (3)$$

where g_c describes the "g = 1.94" signal observed for the [4Fe–4S] cluster in the 1+ oxidation state; typical g values would be g_x = 1.90, g_y = 1.93, and g_z = 2.03 as observed for SiR^{2-}–CO.[8] Since $\tilde{\mathbf{g}}_c$ is quite isotropic and since the orientation of $\tilde{\mathbf{g}}_c$ relative to the siroheme is unknown, we simply use $\tilde{\mathbf{g}}_c = 2$. (This introduces an uncertainty of less than 5% in the final parameters.)

Next we consider exchange interactions between the heme iron and the iron–sulfur cluster. To date, the nature of the linkage between the cluster and the siroheme is not known. However, this linkage seems to be present in all states of SiR for which information about coupling has been obtained.[3,5,6,8] It is reasonable to assume that the observed exchange interactions result from a chemical link, by some intervening ligand, between the siroheme iron and one iron site (designated site 1) of the [4Fe–4S] cluster. We describe the exchange interaction by

$$\hat{H}_{ex} = k_{1h}(\vec{\mathbf{S}}_1\cdot\vec{\mathbf{S}}_h) \quad (4)$$

where S_1 is the (local) spin of cluster site 1. For the calculations in our model we have to evaluate matrix elements of $\vec{\mathbf{S}}_1$ within the ground doublet (eigenstates $|S_cM_c\rangle$) of the iron–sulfur cluster. By using the Wigner–Eckart theorem we can express these matrix elements by the corresponding elements of the cluster spin S_c. Thus

$$\langle S_cM'_c|\vec{\mathbf{S}}_1|S_cM_c\rangle = F_1\langle S_cM'_c|\vec{\mathbf{S}}_c|S_cM_c\rangle \quad (5)$$

This relation allows us to use $\vec{\mathbf{S}}_c$ instead of $\vec{\mathbf{S}}_1$ in eq 4 and we can write

$$\hat{H}_{ex} = J(\vec{\mathbf{S}}_c\cdot\vec{\mathbf{S}}_h) \quad (6)$$

where $J = F_1k_{1h}$. Without detailed knowledge of the internal spin coupling of the [4Fe–4S] cluster and without identification of site 1, the equivalence factor F_1 is not known. (F_1 can have either sign depending on whether S_1 is oriented parallel or antiparallel to $\vec{\mathbf{S}}_c$. We will give an estimate of $|F_1|$ below.) If the exchange interaction is smaller than the zero-field splitting of the heme (which applies here), the effect of $\hat{H}_{ex}$ will be to couple the ground doublet of the cluster weakly to the heme spin quintet, yielding a coupled system whose energies are roughly determined by the zero-field splitting of the heme. In order to compute the g values of the ground doublet we have to solve

$$\hat{H} = \hat{H}_{ZF} + J(\vec{\mathbf{S}}_h\cdot\vec{\mathbf{S}}_c) + \beta(\vec{\mathbf{S}}_h\cdot\tilde{\mathbf{g}}_h\cdot\vec{\mathbf{H}}) + \beta g_c(\vec{\mathbf{S}}_c\cdot\vec{\mathbf{H}}) \quad (7)$$

We have done this by means of a computer program that diagonalizes the matrix of $\hat{H}$ taken in the basis of the 10 product states $|S_h\alpha,S_cM_c\rangle$, where α labels the eigenstates of $\hat{H}_{ZF}$.

It will be instructive to discuss briefly a solution to eq 7 using a second-order perturbation treatment for nondegenerate states.

(18) A quadrupole doublet of a siroheme superimposed on the magnetically split spectrum of the [4Fe–4S] cluster would be very conspicuous, as can be seen from an inspection of Figure 1 of ref 6. In Figure 3, the feature at 0.95-mm/s Doppler velocity belongs to the low-spin ferrous heme of the "g = 1.94" minority species. We have observed[6] low-spin ferrous sirohemes in all states of SiR which exhibit "g = 1.94" signals.

(19) Butler, W. F.; Johnston, D. C.; Fredkin, D. R.; Okamura, M. Y.; Feher, G. *Biophys. J.* **1980**, *32*, 967–992.

(20) Griffith, J. S. "The Theory of Transition Metal Ions"; Cambridge at the University Press: New York, 1971; p 332.

(21) Zimmermann, R.; Spiering, H.; Ritter, G. *Chem. Phys.* **1974**, *4*, 133–141.

Table I. Spin-Expectation Values and g Values Computed from Eq 7 for $S_h = 2$ and $S_c = {}^1/_2$

J/D	E/D	g_x	g_y	g_z	$\langle S_c\rangle_x$[a]	$\langle S_c\rangle_y$	$\langle S_c\rangle_z$	$\langle S_h\rangle_x$	$\langle S_h\rangle_y$	$\langle S_h\rangle_z$
−0.22	0.079	3.32[b]	4.89	1.96	−0.46	−0.49	−0.44	−0.38	−0.74	−0.05
+1.0	0.075	3.31[c]	4.81	1.93	+0.25	+0.35	−0.10	−0.98	−1.41	−0.39
−0.034	0.072	2.29[b]	2.53	2.00	−0.50	−0.50	−0.50	−0.08	−0.14	−0.002

[a] Spin-expectation values were computed with $H = 10$ mT and $D = 10$ cm^{-1} for the "spin-down"state ϕ_-. [b] Computed for $g_c = 2$ and $g_{hx} = g_{hy} = g_{hz} = 2$. [c] The solution for $J/D > 0$ is more sensitive to $\bar{g}_h$; we have used $g_{hx} = g_{hy} = 2.2$ and $g_{hz} = 2$.

Although this method has not quite the adequate precision for our problem, it offers some useful insights. We assume that $\hat{H}_{ZF} \gg \hat{H}_{ex} \gg$ Zeeman terms, take H_{ZF} as the unperturbed Hamiltonian and consider $\hat{H}_{ex}$ as a perturbation. Since hemes in general have $D > 0$ and $E/D < 0.1$ the heme ground state is essentially the $M_h = 0$ singlet. $\hat{H}_{ex}$ will mix the $M_h = \pm 1$ states into the ground state, and the admixture will be linear in J/D. Since the coupled system has an odd number of electrons, the ground state is a Kramers doublet (eigenvectors ϕ_+ and ϕ_-). The magnetic properties of this doublet can be related in the usual way[20] to a spin Hamiltonian with effective spin $S' = {}^1/_2$,

$$\hat{H} = \beta(\vec{S}'\cdot\tilde{g}\cdot\vec{H}) \tag{8}$$

By computing the matrix elements of the two Zeeman terms of eq 7 within the ϕ_+ and ϕ_- manifold and equating the resulting matrix with that of eq 8, $\tilde{g}$ can be computed. A straightforward calculation, neglecting terms quadratic in E/D and J/D, gives

$$\begin{aligned} g_x &= g_c - 6J/D(1 - 4E/D)g_{hx} \\ g_y &= g_c - 6J/D(1 + 4E/D)g_{hy} \qquad g_z \approx g_c \end{aligned} \tag{9}$$

Equation 9 is a good approximation for $D > 0$, $E/D < 0.1$, $|J| \ll D$, and $\beta H \ll D$. Equation 9 shows that the deviation of $(g_x + g_y)/2$ from $g = 2$ is controlled by J/D whereas the splitting between g_x and g_y is governed by $(E/D)(J/D)$. Thus J/D can be determined from the average of g_x and g_y. From the experimental values $g_x = 3.31$ and $g_y = 4.88$, eq 9 yields $J/D = -0.175$ and $E/D \approx 0.08$ (the condition $|J| \ll D$ is not fulfilled; the exact solution to eq 7 yields $J/D = -0.22$). We can see now why the EPR data suggested an $S = {}^3/_2$ system: the particular value of J/D yields $(g_x + g_y)/2 \approx 4$ which is characteristic for the $M = \pm{}^1/_2$ doublet of an $S = {}^3/_2$ system.

In standard EPR experiments the signs of the g values are not determined. Hence we cannot exclude negative values for g_x and g_y from our solution.[22] Thus, the EPR data allow also a solution for $J/D > 0$. This solution occurs for $J/D = +1.0$ (the perturbation expressions of eq 9, of course, do not hold for $J/D \approx 1$).

We have used a computer program to fit our model to the experimental g values at $g_x = 3.31$ and $g_y = 4.88$. In Table I we have listed the results for two solution sets; besides the g values we have listed the components of the expectation values of $\langle S_c\rangle_i = \langle\phi_-|S_{ci}|\phi_-\rangle$ and $\langle S_h\rangle_i = \langle\phi_-|S_{hi}|\phi_-\rangle$ for the cases where a weak magnetic field is applied along the $i = x, y$, or z axis. Note that the coordinate frame is defined by the zero-field-splitting term of the heme. Inspection of Table I shows that the EPR data can be fitted equally well for $J/D = -0.22$ or $J/D = +1.0$. The correct solution, however, can be deduced from the Mössbauer data.

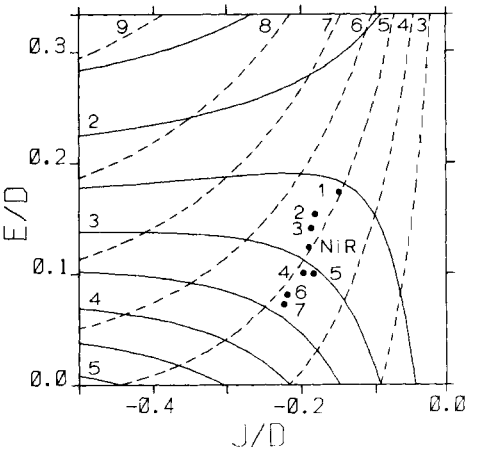

Figure 5. Contours of g_x (solid lines) and g_y (dashed lines) computed by diagonalizing the Hamiltonian of eq 7. The points 1–7 were computed from the g values reported by Janick and Siegel;[8] they correspond to SiR^{2-} to which the following agents were added: KCl, 1 and 2 (two species); KF or KBr, 3; urea, 4; sodium formate, 5; $(Gdm)_2SO_4$, 6; KBr, 7. The data for spinach nitrate reductase (NiR) were taken from ref 12.

As discussed above the internal magnetic fields, $\vec{H}_{int} = -\langle\vec{S}_c\rangle\cdot\tilde{A}/g_n\beta_n$, observed in the 4.2 K Mössbauer spectra of the $[4Fe\text{–}4S]^{1+}$ cluster are essentially the same for SiR^{2-}–CO and the "$g_1 = 4.88$" state of $SiR^{2-}/(Gdm)_2SO_4$ (see Figure 2). For SiR^{2-}–CO the expectation value for the "spin-down" state ϕ_- is $\langle S_{ci}^-\rangle = {}^1/_2$ for $\vec{H}$ along $i = x, y$, or z. According to Table I the solution with $J/D = -0.22$ produces $\langle S_{ci}^-\rangle \simeq -0.5$ whereas the solution with $J/D = +1.0$ produces substantially smaller values for $\langle S_{ci}^-\rangle$. Thus, for $J/D = +1$ one would expect the H_{int} observed for the iron sites of the $[4Fe\text{–}4S]^{1+}$ cluster to be substantially smaller for the "$g_1 = 4.88$" state than for SiR^{2-}–CO, in contrast to experimental observations.

For $J/D < 0$ the value of J/D is rather insensitive to the choice of g_{hx} and g_{hy}, as can be inferred from eq 9. We have therefore used $g_{hx} = g_{hy} = 2$ for the calculations. For $J/D > 0$, on the other hand, the solutions are quite sensitive to the particular choice of g_h. In Figure 5 we have plotted the results of a series of computer calculations for $\beta H \ll D$ (no mixing of excited electronic states into the ground doublet). Shown are the contours of g_x and g_y as functions of E/D and J/D. (Both $D > 0$ and $D < 0$ solutions were considered, hence $0 \le E/D \le {}^1/_3$ covers the whole range of possible E/D values. The $D < 0$ solutions of eq 7 were totally inappropriate and are not shown.) Besides the "$g_1 = 4.88$" species we have analyzed the EPR data of various "$g_1 = 5$" species listed by Janick and Siegel[8] and the data of 2-electron-reduced spinach nitrite reductase.[12] We will discuss these results further in the Conclusion.

We have focused here essentially on g_x and g_y and have paid little attention to the value of g_z, primarily because we lack information of how the cluster is oriented relative to the siroheme. There are two ways to adjust the model to fit the $g_z = 2.07$ resonance. First, one can assume that the cluster is oriented such that the direction of the largest g value of the g_c tensor is along the z direction of g_h. Second, g_z can be increased by increasing g_{hz}. This, however, requires some knowledge about the energies of excited orbital states of the heme (see, for instance, ref 19 and 21).

(22) According to eq 9, g_x and g_y can become negative for $J/D > 0$. However, by redefining the two basis states of the $S = {}^1/_2$ manifold, g_x and g_y can be kept positive; only the sign of the product $g_xg_yg_z$ has physical significance.[23,24] Physically, the two solutions differ as follows. For $J/D = 0$ and $\beta H \to 0$ the heme has no permanent magnetic moment, i.e., $\langle S_h\rangle = 0$, while the "spin-down" state of the cluster has $\langle S_c\rangle^- = -{}^1/_2$. For $J/D \neq 0$ the heme acquires a magnetic moment, $-g_h\beta\langle S_h\rangle \neq 0$. This moment is parallel to that of the cluster for $J/D < 0$ (formally ferromagnetic coupling) and the system, therefore, acquires an increased moment as witnessed by the larger g values. For $J/D > 0$, on the other hand, the moment of the heme opposes that of the cluster, leading initially to a smaller system moment. For $6g_hJ/D = g_c$ the moments of the heme and the cluster cancel each other in the x–y plane (for simplicity, we assume $E/D = 0$); $g_x = g_y = 0$ implies that the ground doublet remains degenerate even in the presence of a (weak) field. Upon further increase of J/D the heme moment dominates; for the "spin-down" state of the system, ϕ_-, we have now $\langle S_h\rangle_x^- < 0$ and $\langle S_c\rangle^- > 0$. In strong applied magnetic field one can determine whether $\langle S_c\rangle^-$ is positive or negative by studying whether the magnetic splittings of the "ferric" or whether those of the "ferrous" cluster sites increase with increasing field.[6] Since only 60% of the material is in the "$g_1 = 4.88$" state, our samples are presently not quite suitable for such studies. However, as pointed out in the text, the solution $J/D \approx +1$ is ruled out by a different argument.

The parameters quoted in Table I were computed for $\beta H \ll D$. (For $\beta H \leq D$ the field will mix excited states into the ground doublet.) We have also performed calculations for magnetic fields corresponding to conditions of X-band EPR spectroscopy. Although $\tilde{\mathbf{g}}$ was found to be quite independent of the field strength for 5 cm^{-1} < D < 15 cm^{-1}, the expectation values of $\langle \tilde{S}_h \rangle$ of the local spin of the heme can be changed substantially by varying the applied field. For $\beta H \ll D$ the ground state behaves like an isolated Kramers doublet with $\langle S_h \rangle^+ = -\langle S_h \rangle^-$. As the field is increased excited states are mixed into the ground doublet and the magnitudes of $\langle S_h \rangle^+$ and $\langle S_h \rangle^-$ become different. Consequently, the hyperfine interactions of the siroheme are different for the ϕ_+ and ϕ_- members of the ground doublet. This, in turn, implies that the ϕ_+ and ϕ_- states should produce different Mössbauer spectra, and quite interestingly, they should yield two different resonances in electron nuclear double resonance spectroscopy (ENDOR). Since $\langle S_h \rangle^+$ and $\langle S_h \rangle^-$ are field dependent whereas $\langle S_c \rangle^+$ and $\langle S_c \rangle^-$ are quite independent of the field strength, one may be able to use ENDOR at different EPR frequencies to distinguish the heme resonances from those belonging to the cluster sites.[17]

In our previous studies we have searched unsuccessfully for excited-state EPR resonances. Our model calculations for $J/D = -0.22$ predict resonances at $g_x = 1.49$, $g_y = 0.49$, and $g_z = 4.11$ for the first excited-state doublet. These resonances would be difficult to detect. First, the state is less populated than the ground state. Moreover, the EPR resonances of the ground doublet broaden significantly above 12 K indicating the onset of fast relaxation. Second, the transition probability at $g_z = 4.11$ is smaller by a factor of 15 than at $g_y = 4.88$ of the ground doublet.

The g values of the "$g = 2.29$" species can easily be fitted with our model. The Mössbauer data, however, suggest strongly that the "$g = 2.29$" species is of a different nature. First, the Mössbauer spectra do not indicate that the heme iron of the "$g = 2.29$" species is high-spin ferrous; rather, an $S_h = 1$ state is suggested. Second, the expectation values of $\langle S_h \rangle$ are too small to account for the observed magnetic splittings. This can be seen by the following considerations: for high-spin ferrous hemes the largest reported values for A_x or A_y are those of reduced cytochrome P450; $A_x/g_n\beta_n = -18$ T and $A_y/g_n\beta_n = -12.5$ T.[25] If we take $A_x/g_n\beta_n = A_y/g_n\beta_n = -18$ T for the siroheme iron of the "$g = 2.29$" species and use the spin expectation values of Table I, we obtain 1.3, −2.3, and ≈0 T for the x, y, and z components of the internal magnetic field, respectively. These values are much too small to account for the observed splittings (we believe that $|H_{int}| > 6.0$ T). If we use a model with $S_h = 1$ we obtain almost identical values for $\langle \tilde{S}_h \rangle$. However, since we have virtually no information about the magnetic hyperfine interactions of hemes with intermediate spin $S_h = 1$, we cannot properly assess whether a similar model with $S_h = 1$ is reasonable.

Complex of SiR with Sulfide. Janick and Siegel[8] have reported optical and EPR spectra of complexes of SiR with sulfide in three oxidation states of the enzyme. The oxidized complex, SiR^0–S^{2-}, displays an EPR signal with g values at $g = 2.24$, 2.21, and 1.96. This set of g values is typical of low-spin ferric isobacteriochlorins.[26] The fully reduced complex, SiR^{2-}–S^{2-}, exhibits a "$g = 1.94$" type signal; thus far it has been proven difficult to prepare this complex at concentrations of more than 0.5 spin/siroheme. A third state, termed "form 2" by Janick and Siegel, is EPR silent; we will show below that it is SiR^{1-}–S^{2-}.

Figure 6B displays a Mössbauer spectrum of SiR^0–S^{2-} taken at 195 K. The spectrum consists of two doublets. The intense doublet, accounting for 80% of the total absorption, belongs to the [4Fe–4S] cluster. The values for $\Delta E_Q = 0.99 \pm 0.03$ mm/s and $\delta = 0.33 \pm 0.02$ mm/s are exactly the same as those observed for the [4Fe–4S] cluster of SiR^0, SiR^{1-}, SiR^0–CN, SiR^{1-}–CN, and SiR^{1-}–NO,[3,5,6] establishing that the cluster is in the 2+ oxidation state. (In general, the electronic ground state of the $[4Fe–4S]^{2+}$ cluster is diamagnetic.) The two absorption lines of the $[4Fe–4S]^{2+}$ cluster are exceedingly sharp, $\Gamma = 0.26$ mm/s full width at half-maximum, despite the fact that four iron sites contribute. The second doublet (indicated by the arrows) has $\Delta E_Q = 2.20 \pm 0.05$ mm/s and $\delta = 0.33 \pm 0.02$ mm/s at 195 K. These parameters are typical of a low-spin ferric heme. Thus both Mössbauer and EPR spectroscopy suggest a low-spin ferric heme.

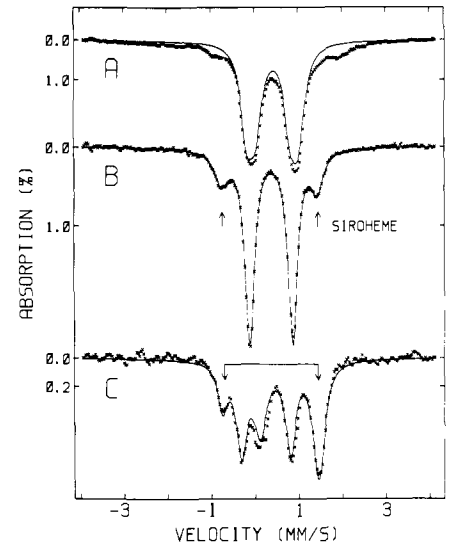

Figure 6. Mössbauer spectra of SiR^0–S^{2-} (A and B) and SiR^{1-}–S^{2-} (C). Part A shows data (crosses) recorded at 4.2 K in a 60-mT parallel field; the solid curve is a simulation of the $[4Fe–4S]^{2+}$ cluster assuming $|A_0| = 2.6$ MHz for each iron site; the curve corresponds to 80% total absorption. (B) Spectrum (crosses) of SiR^0–S^{2-} taken at 195 K in zero field; the solid curve is a least-squares fit constrained by using two quadrupole doublets having areas in the ratio of 1:4. (C) Spectrum (110 K) (crosses) of SiR^{1-}–S^{2-} taken in zero field obtained by subtracting a contribution of 19% SiR^0–S^{2-} from the raw data. The solid curve in C is the sum of a symmetric quadrupole doublet having $\Delta E_Q = 2.15$ mm/s and $\delta = 0.34$ mm/s and a fit to the spectrum of the $[4Fe–4S]^+$ cluster observed for SiR^{2-}–CO. Arrows in B and C indicate the line positions of the siroheme quadrupole doublet.

The spectrum of Figure 6A was recorded at 4.2 K in a parallel field of 60 mT. Two features of this spectrum are noteworthy. First, the quadrupole doublet of the siroheme iron has disappeared and a component with magnetic features has appeared. This is in accord with the expectation from EPR. Second, the absorption lines of the $[4Fe–4S]^{2+}$ cluster are significantly broadened to $\Gamma \approx 0.45$ mm/s. Broadening is not expected since the electronic ground state of $[4Fe–4S]^{2+}$ clusters is diamagnetic. Indeed, no broadening is observed when SiR is in a truly diamagnetic state, as for instance, in SiR^{1-}–CN, where both the siroheme iron and the cluster have $S = 0$.[6] We have discussed earlier[6] for SiR^0–CN that the observed broadening of the cluster absorption lines is caused by magnetic hyperfine interactions, i.e., the iron sites of the cluster are linked to a paramagnetic center. The solid line in Figure 6A is a theoretical spectrum computed with the assumption that the magnetic hyperfine interactions for each of the four iron sites of the cluster can be described by a term $A_0(\tilde{S}\cdot\tilde{I}_i)$, where $S = {}^1/_2$ and $i = 1, 4$. The desired line broadening is obtained for $A_0 \approx 2.6$ Mhz. For SiR^0–S^{2-} we do not have the persuasive evidence for exchange coupling as we have presented for SiR^0.[3] Nevertheless, exchange coupling is suggested for SiR^0–S^{2-} as well. In the following we will strengthen the case for coupling by considering the 1-electron-reduced state.

Figures 6C and 7 show spectra of a reduced sample of SiR–S^{2-}. We have studied the EPR spectra of a sample prepared in parallel with the Mössbauer sample. The spectra suggest that 15–20% of the material is still in the oxidized state. This agrees with the conclusions we have reached from analyses of the Mössbauer

(23) Abragam, A.; Bleaney, B. "Electron Paramagnetic Resonance of Transition Ions"; Charendon Press: Oxford, 1970; p 650.
(24) Huynh, B. H.; Emptage, M. H.; Münck, E. *Biochim. Biophys. Acta* **534**, 295–306.
(25) Champion, P. M.; Chiang, R.; Münck, E.; Debrunner, P. G.; Hager, L. P. *Biochemistry* **1975**, *14*, 4159–4165.
(26) Stolzenberg, A. M.; Strauss, S. H.; Holm, R. H. *J. Am. Chem. Soc.* **1981**, *103*, 4763–4778.

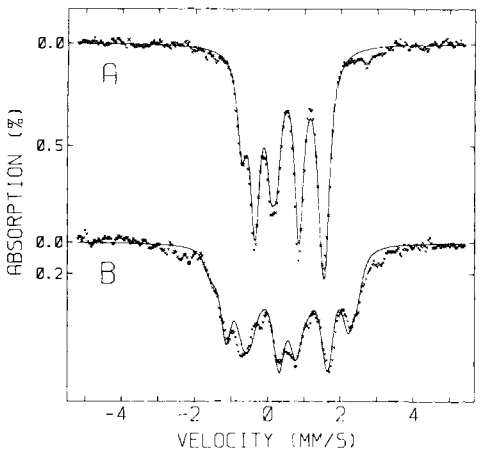

Figure 7. Mössbauer spectra (4.2 K) (crosses) of SiR^{1-}–S^{2-} taken in parallel applied fields of (A) 60 mT and (B) 6.0 T. The solid curves are spectra computed by assuming diamagnetism for all five iron sites. As plotted, the theoretical spectra represent 94% of the observed absorption. The other parameters used for the spectra simulations are as follows: $\Delta E_Q = -2.18$ mm/s, $\eta = 0$, $\delta = 0.36$ mm/s, and $\Gamma = 0.30$ mm/s for the siroheme. For the two irons belonging to site II of the [4Fe–4S] cluster spectrum, $\Delta E_Q = +1.94$ mm/s, $\eta = 0$, $\delta = 0.61$ mm/s, and $\Gamma = 0.30$ mm/s. Contributions of the two site I type irons of the cluster were represented by slightly inequivalent spectra, one with $\Delta E_Q = -0.77$ mm/s and $\delta = 0.46$ m/s and the other with $\Delta E_Q = -0.61$ mm/s and $\delta = 0.54$ mm/s. $\eta = 0.7$ and $\Gamma = 0.28$ mm/s were used for both site I type cluster irons.

spectra. We have subtracted from the raw data a 19% contribution of SiR^0–S^{2-}. The resulting spectra are displayed in Figures 6C and 7. Comparison of the spectra in Figure 6, parts B and C, shows that the quadrupole doublet of the siroheme is essentially unchanged upon reduction and that the doublet of the $[4Fe–4S]^{2+}$ cluster has changed into the four-line pattern of the $[4Fe–4S]^{1+}$ state. In fact, a superposition of the siroheme doublet (20%) of Figure 6B and $[4Fe–4S]^{1+}$ cluster spectrum (80%) of Figure 1 fits the data of Figure 6C very well. (To generate the solid line of Figure 6C we have used the $[4Fe–4S]^{1+}$ cluster spectrum obtained from SiR^{2-}–CO rather than that from SiR^{2-}–CN; the former fits slightly better.) Thus we conclude that the $[4Fe–4S]^{2+}$ cluster of SiR^0–S^{2-} has been reduced by one electron while the siroheme has remained in the low-spin ferric state. We note that the siroheme of SiR–S^{2-} has a lower redox potential than the [4Fe–4S] cluster, in contrast to the relative potentials of all other states studied thus far. In the following we refer to the sample as SiR^{1-}–S^{2-}.

Figure 7A shows a 4.2 K spectrum of SiR^{1-}–S^{2-}. It can be seen that the low-temperature spectrum is essentially the same as that recorded at 110 K. Since both the siroheme and the [4Fe–4S] cluster are in states which normally (i.e., in uncoupled systems) each have an electronic spin $S = {}^1/_2$, one would have expected spectra exhibiting magnetic hyperfine interactions at 4.2 K. This is clearly not the case. There are two possibilities for the absence of magnetic features. First, the relaxation rates of the electronic spins of both the siroheme and the cluster could be fast, leading to averaging out of magnetic effects. This possibility can be eliminated with the aid of the spectrum of Figure 7B. In an applied magnetic field of 6.0 T, magnetic hyperfine interactions will be observed at 4.2 K regardless of whether the spins relax rapidly or slowly, provided that the states are intrinsically paramagnetic (see Chapter II of ref 27). The solid curve in Figure 7B is a theoretical spectrum generated by assuming that both the siroheme iron and the cluster irons reside in diamagnetic environments, an assumption in excellent agreement with the data. This result rules out the possibility of two $S = {}^1/_2$ systems with fast relaxation. The second and appropriate interpretation of the data is that the ground state of SiR^{1-}–S^{2-} is diamagnetic, the diamagnetism resulting from coupling the siroheme spin, $S_h = {}^1/_2$, and the spin of the cluster, $S_c = {}^1/_2$, antiparallel to a resultant spin $S = 0$. This coupling must proceed through exchange interactions rather than by dipolar forces, because dipolar interactions would be easily decoupled in an external field of 6.0 T.

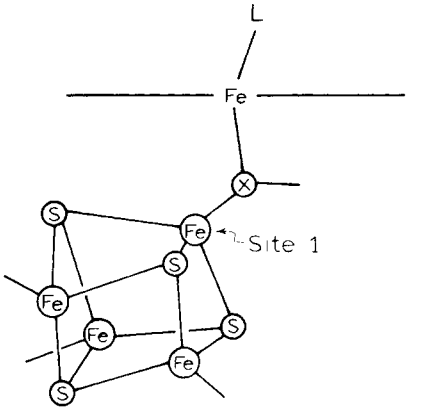

Figure 8. Hypothetical arrangement of the metal centers of SiR. The observation of exchange interactions in all complexation and oxidation states of SiR suggests that the siroheme (shown edge-on) and the iron–sulfur cluster are linked by a bridging ligand X of, as yet, unknown nature. The link could be provided by an amino acid residue (such as cysteinyl sulfur or carboxylate oxygens) or perhaps by an oxo or sulfido ligand. L represents substrates or inhibitors which bind to the heme iron. In some states L may either be absent, a water ligand, or an amino acid residue.

In order to assess the strength of exchange coupling in SiR^{1-}–S^{2-} we offer the following considerations. The Mössbauer spectra show that the siroheme iron is low-spin ferric while the [4Fe–4S] cluster is in the 1+ oxidation state. The latter usually has an $S_c = {}^1/_2$ ground state yielding the "$g = 1.94$" type EPR signal. The spectrum of Figure 7B shows that the system as a whole is diamagnetic at 4.2 K, pointing to the presence of exchange interactions between the heme and the cluster. The physics of this coupling can be described by eq 6 if we assume that $|J|$ is small compared with the crystal field splitting of the heme t_{2g} orbitals and small compared with internal exchange coupling energies of the cluster. Hence our basis states include only the ground doublet of the heme and the ground doublet of the cluster. According to eq 6 we use the cluster spin S_c and an effective coupling constant J. For $J > 0$, the Hamiltonian of eq 6 yields a singlet ground state and an excited triplet state at energy J. With the reasonable assumption that the siroheme iron of SiR^{1-}–S^{2-} is in the same state as in SiR^0–S^{2-} and that the [4Fe–4S] cluster is in the "$g = 1.94$" state which is observed in normal ferredoxins, we have essentially a system with isotropic Zeeman interactions (the g values of the cluster deviate by less than 5% from $g = 2$ while g_x and g_y of the heme are within 12% of 2). Using isotropic Zeeman interactions, $\beta g_h(\vec{S}_h \cdot \vec{H})$ and $\beta g_c(\vec{S}_c \cdot \vec{H})$ for the heme and the cluster, respectively, and using a coupled representation $\vec{S} = \vec{S}_h + \vec{S}_c$, we can write the exchange and Zeeman terms as (using $g_1 = g_2 = 2$)

$$\hat{H} = (J/2)[S(S+1) - {}^3/_2] + 2\beta(\vec{H}\cdot\vec{S})$$

which yields for the energies

$$E(S,M) = (J/2)[S(S+1) - {}^3/_2] + 2\beta HM \qquad (10)$$

where $M = 0$ for the singlet and $M = 0, \pm 1$ for the triplet states. From eq 10 it follows that the $M = -1$ state of the triplet is the ground state if $\beta H > J/2$. Since the $M = \langle S_z \rangle = -1$ state is paramagnetic, this state would be associated with a Mössbauer spectrum exhibiting magnetic hyperfine interactions. The spectrum of Figure 7B shows that the electronic ground state is diamagnetic even for $H = 6.0$ T, i.e., $J > 6$ cm^{-1}.

Conclusions

We have studied here the Mössbauer spectra of SiR^{2-}/$(Gdm)_2SO_4$ and those of SiR complexed with sulfide. In the following we discuss the pertinent results. A schematic representation of the metal center of SiR is suggested in Figure 8.

We have shown above that the siroheme iron of SiR^{2-}/$(Gdm)_2SO_4$ (referred to as the "$g_1 = 4.88$" species) has Mössbauer

parameters typical of a high-spin ferrous heme. This observation is interesting for a variety of reasons. First, it shows that a high-spin ferrous siroheme has Mössbauer parameters very similar to those observed for other high-spin ferrous porphyrins, such as iron(II) protoporphyrin IX[16] or iron(II) chlorin.[28] Second, the recognition of a high-spin ferrous (S_h = 2) heme in SiR^{2-}/$(Gdm)_2SO_4$ has provided us with a crucial piece of information for the development of the exchange coupling model which we have presented in the Results section. Third, this observation sheds some light on the nature of the heme iron of 1-electron-reduced SiR, SiR^{1-}. In the latter state the siroheme has ΔE_Q = 1.90 mm/s at 4.2 K which fits well to a high-spin ferrous state; however, the isomer shift, δ = 0.62 mm/s, is clearly outside of the high-spin ferrous range. We have therefore suggested,[5] essentially by eliminating S_h = 2 and S_h = 0, that the siroheme iron of SiR^{1-} is intermediate spin, S_h = 1. The results obtained here strengthen this suggestion.

We have shown here that the g values of "g_1 = 5" type species do not result from an $S = {}^3/_2$ state, despite the fact that the EPR data fit quite well to such a system. The Mössbauer data, however, are in conflict with such an assignment. Our model calculations show that the similarity of the g values with those observed for $S = {}^3/_2$ systems is fortuitous; a particular value for J/D yields $(g_x + g_y)\ 2 \approx 4$.

According to our model two parameters can be readily extracted from the EPR experiments: g_x and g_y determine the rhombicity parameter of the siroheme, E/D, and the ratio J/D. Inspection of Figure 5 shows that all "g_1 = 5" type species observed thus far[8] cluster around $J/D = -0.2$ within a rather narrow range. The same value for J/D fits also the EPR data of 2-electron-reduced spinach nitrite reductase.[12] J/D is well defined for a given species, as witnessed by the relatively sharp EPR lines. For instance, the g_y = 4.88 resonance of SiR^{2-}/$(Gdm)_2SO_4$ has a width of 8 mT; this yields a variance of ±0.005 for J/D.

With a good value of J/D available we need an estimate of D. Further, we also have to discuss how the effective J values are related to the parameter k_{1h} (see eq 4) which characterizes the linkage between the cluster and the siroheme iron. Thus far, the value of D of the "g_1 = 4.88" species is unknown,[29] and to date, D values of only two high-spin ferrous hemes have been reported. High-field Mössbauer studies of reduced cytochrome P450 from *Pseudomonas putida*[25] and of the model complex[30] (*meso*-tetraphenylporphinato)bis(tetrahydrofuran)iron(II)) have yielded $D \approx 15$ and 6 cm^{-1}, respectively. (From magnetic susceptibility studies of deoxymyoglobin a value of $D \approx 5$ cm^{-1} has been deduced;[31] there is, however, evidence that the spin Hamiltonian eq 1 does not satisfactorily describe the ground manifold of myoglobin.[32]) Using the reported values for D we obtain an estimate $-J \approx 1$–3 cm^{-1} for the "g_1 = 5" species of SiR.

In eq 4 we have defined the coupling constant k_{1h}. This parameter characterizes the bond between the cluster and the siroheme iron and is related to the effective coupling constant J by $J = k_{1h}F_1$, eq 5 and 6, where F_1 is an equivalence factor which depends on the electronic structure of the iron–sulfur cluster. We can estimate F_1 by comparing the magnetic hyperfine interactions of the cluster in the "g = 1.94" state with those of oxidized and reduced rubredoxin. Let us assume that one can describe the exchange interactions among the four iron atoms of the cluster with a simple Heisenberg Hamiltonian, as used by Papaefthymiou et al.[33] for the evaluation of magnetic susceptibility data. For reduced [2Fe–2S] ferredoxins[34,35] and oxidized [3Fe–4S] clusters[36] such a Hamiltonian has successfully explained a variety of experimental observations.[37] In such a spin-coupling model the magnetic hyperfine interactions of the four iron sites, i = 1–4, can be computed by evaluating the expressions $\vec{S}_i \cdot \tilde{A}_i \cdot \vec{I}_i$ within the system ground doublet $|S_c M_c\rangle$. Evaluation of these matrix elements would proceed by using eq 5 and, thus, the same factors F_i would connect the A tensors of the coupled representation A_i^c with those of the uncoupled representation, $A_i^c = F_i A_i$. (In the language of a vector-coupling model the F_i are factors which project the local spins onto the direction of the system spin. For reduced [2Fe–2S] clusters the F_i have the well-known numerical values ${}^7/_3$ and ${}^{-4}/_3$.)

It has been well established that some $[4Fe–4S]^+$ clusters display two pairs of equivalent iron sites, labeled sites I and II (for a discussion see ref 6 and 13). Site I is ferric in character and has a fairly isotropic A tensor; A = (−31.5, −33.5, −33.5) MHz for SiR^{2-}–CO. Site II is ferrous in character and has more anisotropic magnetic hyperfine interactions; A = (+22.0, +11.0, +19.2) MHz.[6] Very similar parameters have been reported for the reduced ferredoxin from *Bacillus stearothermophilus*.[13] Rubredoxin, which has a single iron atom in a tetrahedral environment of sulfur ligands and is therefore an appropriate model, has A = (−22.2, −21.5, −22.8) MHz in the ferric state, and A = (−27.6, −11.3, −51.7) MHz in the ferrous state.[39] By comparing the average A values of sites I and II with those of ferric and ferrous rubredoxin, respectively, we obtain $F_I = +1.5$ and $F_{II} = -0.6$. With these estimates we obtain for the range of k_{1h} values $0.5\ cm^{-1} < |k_{1h}| < 5\ cm^{-1}$. The preceeding considerations show that the sign of J does not reveal whether the exchange coupling is ferromagnetic ($k_{1h} < 0$) or antiferromagnetic ($k_{1h} > 0$), since we do not know whether the cluster is attached to the siroheme iron at an iron of site I or site II type.

Sulfide is the product of the 6-electron reduction of SO_3^{2-} catalyzed by SiR. Rueger and Siegel[40] have reported stopped-flow data which suggest that S^{2-} dissociation from the enzymes may be rate limiting in catalysis. Our studies of the complex of SiR with sulfide have yielded two interesting results. First, our data show conclusively that upon reduction of SiR^0–S^{2-} the first electron is accommodated by the iron–sulfur cluster; this is in contrast to all other states of SiR where the siroheme is first reduced. Thus upon complexation of sulfide, the heme attains a state with a lower redox potential than that of the cluster.[41] Second, 1-electron-reduced SiR–S^{2-} has a diamagnetic electronic ground state re-

(27) Münck, E. In "The Porphyrins", Dolphin, D., Ed.; Academic Press: New York, 1979; Vol. 4, pp 379–423.
(28) Huynh, B. H.; Lui, M. C.; Moura, J. J. G.; Moura, I.; Ljundahl, P. O.; Münck, E.; Payne, W. J.; Peck, H. D., Jr.; DerVartanian, D. V.; LeGall, J. *J. Biol. Chem.* **1982**, *257*, 9576–9581.
(29) In principle, one could determine D by measuring the temperature dependence of the "g_1 = 5" EPR signals and fitting the data to the energy level scheme of Figure 4. Unfortunately, the EPR spectra broaden significantly above 10–15 K rendering such determinations of D very difficult. It may be possible to determine D by studying the relaxation behavior of the EPR spectra.
(30) Boso, B.; Lang, G.; Reed, C. *J. Chem. Phys.* **1983**, *78*, 2561–2567.
(31) Nakano, N.; Otsuka, J.; Tasaki, A. *Biochim. Biophys. Acta* **1971**, *236*, 222–233.
(32) Kent, T. A.; Spartalian, K.; Lang, G.; Yonetani, T.; Reed, C. A.; Collman, J. P. *Biochim. Biophys. Acta* **1979**, *580*, 245–258.
(33) Papaefthymiou, G. C.; Laskowsky, E. J.; Frota-Pessoa, S.; Frankel, R.; Holm, R. H. *Inorg. Chem.* **1982**, *21*, 1723–1728.
(34) Münck, E.; Debrunner, P. G.; Tsibris, J. C. M.; Gunsalus, I. C. *Biochemistry* **1972**, *11*, 855–863.
(35) Dunham, W. R.; Palmer, G.; Sands, R. H.; Bearden, A. J. *Biochim. Biophys. Acta* **1971**, *253*, 373–384.
(36) Kent, T. A.; Huynh, B. H.; Münck, E. *Proc. Natl. Acad. Sci. U.S.A.* **1980**, *77*, 6574–6576.
(37) The coupling models for reduced [2Fe–2S] centers and oxidized [3Fe–4S] clusters are fairly straightforward, primarily because the oxidation states of the various iron sites were identified by Mössbauer spectroscopy to be either typical high-spin Fe^{3+} or typical high-spin Fe^{2+}. [3Fe–4S] clusters in the reduced state[38] and [4Fe–4S] clusters, on the other hand, have much more delocalized structures, and it is not quite clear what values one should use for the local spins S_i. Further, the $[4Fe–4S]^+$ cluster is formally $3Fe^{2+}$ and $1Fe^{3+}$ whereas the Mössbauer data (see ref 6 and Figures 1 and 7A) suggest two pairs of identical sites.
(38) Huynh, B. H.; Moura, J. J. G.; Moura, I.; Kent, T. A.; LeGall, J.; Xavier, A. V.; Münck, E. *J. Biol. Chem.* **1980**, *255*, 3242–3244.
(39) Schulz, C.; Debrunner, P. G. *J. Phys., Colloq.* (*Orsay, Fr.*) **1976**, *37*, Suppl. C6, 153–158.
(40) Rueger, D. C.; Siegel, L. M. "Flavins and Flavoproteins", Singer, T. P. Ed.; Elsevier: Amsterdam, 1976; pp 610–620.
(41) According to the EPR data[8] the potentials of the two centers differ by at least 100 mV in the S^{2-}-ligated enzyme. Since in unligated SiR the heme potential is 65 mV more *positive* than that of the [4Fe–4S] cluster, the addition of S^{2-} to the enzyme alters the relative potentials of the center by 165 mV. The effect of S^{2-} is in marked contrast to that of CN^-, which on binding to SiR shifts the heme potential some 180 mV more positive and the [4Fe–4S] potential 90 mV more negative than in the unligated enzyme.[2,4]

sulting from exchange interactions between the $S_h = {}^1/_2$ ground state of the low-spin siroheme and the $S_c = {}^1/_2$ state of the cluster. This coupling is antiferromagnetic in the sense that the electron spins of the heme and the cluster are coupled antiparallel. However, since we do not know whether the cluster is attached at site I or site II to the siroheme, the sign of the factor F_I is unknown and, thus, the sign of k_{1h} is undetermined, as in $SiR^{2-}/(Gdm)_2SO_4$. By studying SiR^{1-}–S^{2-} in a strong applied field we have determined that $J > 6$ cm^{-1}.

It is interesting to note that the signs of J are different for $SiR^{2-}/(Gdm)_2SO_4$ and for SiR^{1-}–S^{2-}. Since $J = k_{1h}F_1$, both k_{1h} and F_1 determine its sign. It is clear from the Mössbauer data that the iron–sulfur cluster is in the same state in both complexes. Therefore, we consider it unlikely that the link between the cluster and the siroheme has switched from a type I site to a type II site between the two complexes under discussion. This, then, suggests that the signs of k_{1h} differ between the two complexes, i.e., the coupling is ferromagnetic in one complex and antiferromagnetic in the other. It is not surprising that the exchange interactions between the heme and the cluster are different in the two complexes because the low-spin ferric heme of SiR^{1-}–S^{2-} has one unpaired d-electron whereas the high-spin ferrous iron of $SiR^{2-}/(Gdm)_2SO_4$ has four. Thus, the two complexes can develop quite different exchange pathways.

We have discussed in the Results section that the g values of the "$g = 2.29$" species can be fitted with the model developed for $SiR^{2-}/(Gdm)_2SO_4$. Our present evidence suggests that the the siroheme of the "$g = 2.29$" species is not high-spin ferrous, although our data do not strictly rule out such an assignment. It appears that the siroheme of the "$g = 2.29$" species is in a state more closely related to that of SiR^{1-} than that of the "$g_1 = 5$" species. The optical data, however, give quite a different picture. Janick and Siegel[8] have shown that the UV/vis spectra of the "$g = 2.29$" and the "$g_1 = 5$" species are virtually identical and quite distinct from that of SiR^{1-}. Since the optical spectra were recorded at room temperature and the EPR and Mössbauer data were obtained at temperatures below 200 K, the possibility of a spin transition of the siroheme iron has to be considered. Low-temperature optical studies are in preparation.

In conclusion, we have analyzed the EPR and Mössbauer data of $SiR^{2-}/(Gdm)_2SO_4$ and complexes with sulfide, and we have demonstrated exchange coupling between the siroheme and the iron–sulfur cluster. Thus far, we have provided evidence for exchange coupling in eight different states of SiR. In this study we have been able, for the first time, to determine the strength of the coupling. It is clear that the magnitude and signs of J vary noticeably between the different states (see also ref 5), indicating that different exchange pathways are utilized. We have presented here and elsewhere models for the description of the exchange coupling which should provide a framework for further explorations of this unique arrangement of prosthetic groups.

Acknowledgment. This work was supported by NIH Grants GM-32210 (to L.M.S.) and GM-22701 (to E.M.), NSF Grant PCM-83-06964 (E.M.), and Veterans Administration Project Grant 7875-01 (to L.M.S.).

Registry No. NADPH-sulfite reductase, 9029-35-0; siroheme, 52553-42-1; sulfide, 18496-25-8.

Metal Alkoxides—Models for Metal Oxides. 4.[1] Alkyne Adducts of Ditungsten Hexaalkoxides and Evidence for an Equilibrium between Dimetallatetrahedrane and Methylidynemetal Complexes: $W_2(\mu\text{-}C_2H_2) \rightleftharpoons 2W{\equiv}CH$

Malcolm H. Chisholm,* Kirsten Folting, David M. Hoffman, and John C. Huffman

Contribution from the Department of Chemistry and Molecular Structure Center, Indiana University, Bloomington, Indiana 47405. *Received January 24, 1984*

Abstract: In the presence of pyridine, alkyne adducts of ditungsten hexaalkoxides of formula $W_2(OR)_6(\mu\text{-}C_2R_2')(py)_n$, where R = *t*-Bu, R′ = H, and n = 1, R = *i*-Pr, R′ = H, and n = 2, and R = CH_2-*t*-Bu, R′ = Me, and n = 2, have been isolated and characterized by variable-temperature NMR studies and single-crystal X-ray crystallography. In each compound there is a pseudotetrahedral $W_2(\mu\text{-}C_2)$ core with C–C distances (1.38–1.44 Å) and W–W distances (2.57–2.67 Å) that are approaching those of C–C and W–W single bonds. This implies a substantial rehybridization of triple bonds toward the idealized dimetallatetrahedrane in the reaction $(RO)_3W{\equiv}W(OR)_3 + R'C{\equiv}CR' \rightarrow (RO)_6W_2(C_2R'_2)$. Steric factors are important in controlling both the length of the W–W and C–C bonds of the central $W_2(\mu\text{-}C_2R'_2)$ moiety and the geometry about the tungsten atoms. Counting the $\mu\text{-}C_2R_2$ ligand to occupy one coordination site to each metal, the structure of the *tert*-butoxy compound is based on two fused trigonal-bipyramidal moieties sharing a common equatorial (C_2R_2) and axial (OR) edge; the neopentoxide has tungsten atoms that share an edge of a trigonal bipyramid and an octahedron and the isopropoxide has two octahedral tungsten atoms fused along a common face formed by two O-*i*-Pr ligands and the $\mu\text{-}C_2H_2$ ligand. All three compounds are fluxional on the NMR time scale though low-temperature limiting spectra consistent with expectations based on the structures found in the solid state are observed. Labeling studies, involving $H^{13}C^{13}CH$ and $D^{12}C^{12}CD$, suggest that the ethyne adduct $W_2(O\text{-}t\text{-}Bu)_6(\mu\text{-}C_2H_2)(py)$ is in equilibrium with $(t\text{-}BuO)_3W{\equiv}CH$. These studies are compared with related studies by Cotton and Schrock and their co-workers who have previously noted the formation of alkylidyne ligands in the reactions between $W_2(O\text{-}t\text{-}Bu)_6$ and disubstituted alkynes RC≡CR where R = alkyl and phenyl. (i) Crystal data for $W_2(O\text{-}t\text{-}Bu)_6(\mu\text{-}C_2H_2)(py)\cdot{}^1/_2py$ at −160 °C: a = 17.399 (5) Å, b = 11.336 (3) Å, c = 11.216 (3) Å, α = 71.53 (1)°, β = 113.72 (1)°, γ = 98.90 (2)°, Z = 2, d_{calcd} = 1.714 g cm^{-3}, and space group $P\bar{1}$. (ii) Crystal data for $W_2(O\text{-}i\text{-}Pr)_6(py)_2(\mu\text{-}C_2H_2)$ at −165 °C: a = 19.061 (11) Å, b = 15.674 (7) Å, c = 12.234 (5) Å, β = 108.08 (1)°, Z = 4, d_{calcd} = 1.737 g cm^{-3}, and space group $P2_1/a$. (iii) Crystal data for $W_2(OCH_2\text{-}t\text{-}Bu)_6(\mu\text{-}C_2Me_2)(py)_2$: a = 37.822 (21) Å, b = 12.207 (5) Å, c = 22.163 (9) Å, β = 101.01 (2)°, Z = 8, d_{calcd} = 1.459 g cm^{-3}, and space group $C2/c$.

In this series of papers we are (i) examining structural and bonding relationships between metal oxides and metal alkoxides and (ii) investigating the chemistry of metal–carbon bonds supported by alkoxy ligands.[2] Previously, we reported[3] studies of

0002-7863/84/1506-6794$01.50/0 © 1984 American Chemical Society